Amino acids promote black carbon aggregation and microbial colonization in coastal waters off Vietnam

Mar Benavides, Thuoc Chu Van, Xavier Mari

Amino acids promote black carbon aggregation and microbial colonization in coastal waters off Vietnam

[1,]Mar Benavides, [2]Chu Van Thuoc, [1,2,3]Xavier Mari*

[1]Aix Marseille Univ, Université de Toulon, CNRS, IRD, MIO UM 110, 13288, Marseille, France

[2]Institute of Marine Environment and Resources (IMER), Vietnam Academy of Science and Technology (VAST), 246 Da Nang Street, Haiphong, Vietnam

[3]University of Science and Technology of Hanoi (USTH), Vietnam Academy of Science and Technology (VAST), Hanoi, Vietnam

*corresponding author: Mar Benavides mar.benavides@ird.fr

Abstract

The combustion of fossil fuels and biomass produces pyrogenic organic matter usually known as 'black carbon' (BC), which are transported across the atmosphere as particulate aerosol, eventually deposited on land and oceans. Soil studies have investigated the potential microbial colonization and remineralization of BC particles, but this process has been seldom studied in marine waters. BC provides a significant input of organic carbon to the oceans, yet its fate and role in its biogeochemical cycling remains unknown. Here we explored the microbial colonization of BC particles in coastal seawater samples collected in Halong Bay (northern Vietnam). Using high-resolution mass spectrometry and microscopy methods, we observed an increasing colonization of BC particles by marine microbes in the presence of amino acids. Our results suggest that natural organic matter (NOM) present in seawater may promote the microbial colonization and eventual remineralization of BC particles. Future experiments should explore the potential microbial remineralization of BC particles to unveil the role of this massive source of carbon to coastal marine ecosystems.

Keywords: pyrogenic organic matter; nanoSIMS; SEM; aggregates; Halong Bay

1. Introduction

The ability of the oceans to sequester CO_2 depends on organic particle production via photosynthesis and their microbial remineralization in the water column. If sinking organic particles are remineralized by microbial activity in shallow waters the resulting CO_2 is released back to the atmosphere, whereas if they reach depths deep enough to avoid release of CO_2 back to the atmosphere net carbon sequestration takes place. The balance between these two processes determines the effectiveness of CO_2 sequestration by the ocean, a process known as the biological carbon pump.

Black carbon (BC) is pyrogenic (i.e. thermally altered) organic matter produced during incomplete combustion of fossil fuels, biofuels and biomass, which is an unaccounted-for source of carbon in marine ecosystems. BC is emitted to the atmosphere at an estimated rate of 2 to 29 Tg per year (Bond et al., 2013), and is deposited onto land and ocean surfaces via dry and wet deposition. Deposition rates are estimated at ~12 Tg C per year on the ocean (Jurado et al., 2008) and ~5 Tg C per year on land (McBeath et al., 2015). In addition to direct atmospheric input of BC to the ocean, a fraction of the BC deposited on land can reach the coastal ocean via riverine runoff. Estimates of the fluvial flux of BC to the coastal ocean vary widely from 8 to 37 Tg C per year (Coppola et al., 2018a), exceeding the estimated deposition of BC on land. While BC impacts the global ocean as a whole, its effects are likely aggravated in coastal zones which receive BC via atmospheric deposition summed to riverine runoff. The coastal ocean only accounts for 10% of the global ocean surface, but supports nearly 20% of marine primary production (Del Giorgio and Duarte, 2002) and contributes about ~30% of the CO_2 sequestered by the oceans on a global scale (Borges et al., 2005). Hence, the effect of BC on coastal ocean carbon cycling needs to be elucidated.

Due to their porous structure (Rockne et al., 2000; Zerda et al., 2000) and surface coverage with oxygen-containing functional groups (Masiello, 2004), BC particles are highly

reactive (Liang et al., 2006) and have been observed to adsorb natural organic matter (NOM) and nutrients from seawater (Mari et al., 2014, 2017). The interaction between BC and microbes may impact the biological carbon pump in two ways: (i) the adsorption of NOM and nutrients onto BC particles decreases the concentration of these solutes in seawater limiting growth and activity of marine microbes, and/or (ii) NOM-enriched BC particles attract microbes with particle-attached lifestyles promoting particle degradation (Weinbauer et al., 2012). BC may thus impact marine carbon cycling significantly (Weinbauer et al., 2017), however most of our knowledge on the interaction between BC and microbes comes from soils studies, while fewer have sought to find the fate of these particles at sea (Cattaneo et al., 2010a; Mari et al., 2014; Pradeep Ram et al., 2018).

Atmospheric BC particles deposited on land through wet or dry deposition are known to alter microbial activity in soils (Liang et al., 2010), affecting the efficiency of NOM degradation (Wu et al., 2017). BC particles (reference material or naturally deposited particles) added to seawater are rapidly colonized by bacteria, resulting in an enhancement of particle-attached bacterial production (Malits et al., 2015; Mari et al., 2014). Here we investigated whether microbial colonization of BC particles in the presence of amino acids. Using nanoscale secondary ion mass spectrometry (nanoSIMS) and microscopy methods, we document an increasing colonization of BC particles with time over 48 h.

The projected increase in BC deposition in the coming years (OECD, 2016), which is especially acute in Asia, calls for the urgent need of understanding how it affects marine microbial communities, which are behind all major element cycles sustaining life in the oceans (carbon, nitrogen, phosphorus, sulfur), and have a crucial role in determining the ocean's ability to regulate global climate. While the metabolic processes behind the bacterial colonization and degradation of BC, and the extent to which these contribute to the biological carbon pump are currently unknown, our results provide a step forward on our understanding

of BC-microbial interactions in the ocean.

2. Materials and methods

2.1. Sampling and experimental setup

Samples were taken from Halong Bay in the northern coast of Vietnam on 6 November 2018 using a small boat. Surface seawater was collected with a hydrochloric acid-cleaned bucket from the side of the boat. Surface microlayer (SML) samples were collected from the bow of the boat (1 m above sea level) using a 40 x 25 cm glass plate sampler vertically dipped and slowly withdrawn. The SML adhering to the glass plate was collected into Nalgene bottles (Cunliffe and Wurl, 2014). Each plate dip recovers about 8 mL of SML, so the plate was dipped about 75 times to obtain 600 mL.

The obtained 600 mL of SML were mixed with 5400 mL of surface seawater (11.11% v/v). BC reference material obtained from diesel combustion (Sigma Aldrich NIST2975) was added to a final concentration of 0.16 g L^{-1}, which is representative of the BC concentrations found in sea surface slicks (Mari et al., 2014). We note however that BC deposited in the ocean is a mix of several combustion sources, and hence the reference material used here only represents 'natural' BC inputs partially. On top of the reference BC material added, background 'natural' BC may have been present in our samples. While we did not measure BC concentrations in our samples, previous studies have reported highly variable concentrations in the SML ranging from 8 to 25610 µM C (Mari et al., 2017).

The seawater, SML and BC mix was distributed in fifteen 250 mL transparent polycarbonate bottles. Three sets of triplicates were amended with a mix containing >20 algal amino acids labelled with ^{15}N (98 atom%, Sigma Aldrich catalogue no. 608947). This mix was added to represent 10% of usual in situ dissolved organic nitrogen concentrations (i.e., between 5 and 38 µmol L^{-1}; Mari et al., 2017). Each triplicate set of isotope-amended bottles

were incubated for 12, 24 and 48 h in a stirring plate placed inside an MLR 351 Sanyo Versatile Environmental Test Chamber programmed to mimic the in situ diel light cycle (10:17 hours of light and 11:29 hours of darkness) and surface seawater temperature (28ºC). Two sets of unamended triplicates were used as 'time zero' (not incubated), and 'control' (48 h incubation without ^{15}N-labeled amino acid amendments). Each bottle was filtered onto 0.2 µm polycarbonate filters, fixed with 4% paraformaldehyde (final concentration) for 1 h at room temperature and stored at -20ºC. The filters were used for microscopy and nanoscale secondary ion mass spectrometry (nanoSIMS) analyses as outlined below.

2.2. NanoSIMS

Circles of 1 cm diameter were excised from the polycarbonate filters and placed onto nanoSIMS sample holders. The analyses were performed using a N50 nanoSIMS (Cameca, Gennevilliers, France) at the French National Ion MicroProbe Facility according to previously described methods (Benavides et al., 2017). A 1.3 to 3 pA 16 keV Cesium (Cs^+) primary beam focused onto ~100 nm spot diameter was scanned on a 256 x 256 pixel raster with a raster area of 20 x 20 µm, and a counting time of 1000 µs per pixel. Samples were pre-sputtered with Cs^+ for 250 sec to remove surface contaminants and increase conductivity. Negative secondary ions $^{12}C^-$, $^{12}C^{14}N^-$, $^{12}C^{15}N^-$ and $^{31}P^-$ were detected with electron multiplier detectors, and secondary electrons were simultaneously imaged. Fifteen serial quantitative secondary ion mass planes were generated and accumulated to the final image. Mass resolving power was ~8000 in order to resolve isobaric interferences. Data were processed using the LIMAGE software (L. Nittler, Carnegie Institution of Washington, https://sites.google.com/carnegiescience.edu/limagesoftware/). All scans were corrected for any drift of the beam during acquisition. Isotope ratio images were generated by dividing the $^{13}C^-$ ion count by the $^{12}C^-$ ion count, and the $^{12}C^{15}N^-$ ion count by the $^{12}C^{14}N^-$ ion count. ^{15}N-

101 enriched areas were selected as regions of interest (ROI). For each ROI, the $^{15}N/^{14}N$ ratios
102 were calculated. The number of ROIs analyzed were 60 per control (non ^{15}N-amended)
103 sample and 110 for ^{15}N-labeled samples.
104
105 *2.3 Cell counts*
106 Each polycarbonate filter was stained with 1 µg mL^{-1} 4′,6-diamidino-2-phenylindole
107 solution (DAPI) to determine bacterial abundance using an epifluorescence microscope
108 (Zeiss Axioplan, Jana, Germany) fitted with a 352-402 nm excitation filter.
109
110 2.4. *Scanning electron microscopy (SEM) analyses*
111 The samples of the nanoSIMS experiments (above) were used for SEM imaging after gold
112 sputtering for 10 minutes at 15mA on an Edwards S150B sputter coater apparatus. Imaging
113 was carried out on a FEI Teneo running in high vacuum, at 20 kV and using the built-in
114 Everheart Thornley detector for secondary electrons.
115
116 **3. Results**
117 Over the course of our experiment, we observed an increasing adsorption of ^{15}N-labeled
118 amino acid and microbial colonization on BC particles. Visual examples of this are shown in
119 the nanoSIMS images of Fig. 1. The morphology of the BC particles is depicted by ^{12}C
120 counts (Figs. 1A-D). We observed an increase in ^{15}N-labeled amino acid adsorption onto BC
121 particles with incubation time, as depicted by the increasing ^{15}N-enrichment from 12 to 48 h
122 (Figs. 1E-H). The increasing ^{15}N-enrichment of BC particles was paralleled by an increased
123 presence of bacteria, as proxied by ^{31}P-enrichment (Figs. 1I-L).
124 The average isotope enrichment values for controls and samples incubated with ^{15}N-
125 labeled amino acids at 12, 24 and 48 h are shown in Fig. 2. The $^{15}N/^{14}N$ ratio of the BC

126 particles analysed increased significantly from 0.07 to 3.5 between 12 and 48 h as compared
127 to the control (one-way ANOVA $p<0.05$; Fig. 2A). We observed a 97% increase in ^{31}P
128 enrichment at 24 h and of 99% at 48 h (Fig. 2B), coinciding with a 60 and 76% increase in
129 bacterial abundance as depicted by DAPI counts at 24 h and 48 h, respectively (Fig. 2C). ^{31}P-
130 enrichment values and bacterial DAPI counts were positively and significantly correlated (r^2
131 $= 0.98$, $p<0.05$).
132 Colonizing bacteria were not spotted in SEM images of control samples (not incubated
133 with ^{15}N-labeled amino acids; Fig. 3A), while those amended with amino acids showed
134 colonizing bacterial assemblages as biofilms covering BC particles (Figs. 3B-C).
135
136 **4. Discussion**
137 BC particles provide a substantial input of organic carbon to the oceans, yet their fate
138 and its interactions with the marine biota are unknown. BC was long thought to be strictly
139 refractory and thus unavailable for microbial processing (Masiello, 2004). However, BC
140 particles have a fractal morphology which confers them a high specific surface area and
141 highly adsorptive properties. Such characteristics render BC particles useful for agricultural
142 soil treatments to enhance nutrient and water retention (Gao et al., 2019). Recent studies have
143 shown that at least a fraction of BC can be microbially degraded in soils, but the degree of
144 degradation may vary with BC origin (source material), combustion temperature, pH, as well
145 as the diversity and activity of the *in situ* microbial community (Zimmerman, 2010).
146 The microbial degradation of BC particles in soils may be enhanced or decreased
147 according to the availability of other substrates such as labile NOM or nutrients (Hamer et al.,
148 2004). The so-called 'priming effect' refers to the stimulation (positive priming) or
149 suppression (negative priming) of BC mineralization in the presence of organic or inorganic
150 substrates. While this effect has been documented in soil studies (Hamer et al., 2004),

151 whether it also takes place in marine waters or how it may affect the biological carbon pump
152 is unknown (Weinbauer et al., 2012). Here we observed an increase in BC-associated bacteria
153 of up to 76% over 48 h incubation in the presence of ^{15}N-labeled amino acids (Fig. 2C). Our
154 results are in agreement with previous incubation experiments where following BC addition
155 to seawater, a decrease in bulk dissolved organic carbon concentrations accompanied by an
156 increase in BC particle-attached bacterial production and abundance was observed (Cattaneo
157 et al., 2010b; Mari et al., 2014). Similarly, other studies observed a rapid bacterial
158 colonization of BC reference material in seawater, increasing from 10-25% after ~30 min to
159 >40% after 24 h (Cattaneo et al., 2010a; Weinbauer et al., 2009). These studies identified the
160 increased particle-attached microbial abundance and activity as a response to NOM
161 adsorption onto BC surfaces.
162 The microbial colonization of BC will depend on the particle's surface reactivity and
163 porosity, which determine the interactions with bacterial cell surface components (Hill et al.,
164 2019). Mari et al. (2014) observed that BC enhances aggregation processes and the transfer
165 of dissolved organic carbon to the particulate phase. Cattaneo et al. (2010a) observed that the
166 microbial colonization of BC-induced aggregates increases linearly with particle size. In our
167 experiments we observed a clear increase in aggregation in samples amended with ^{15}N-
168 labeled amino acids as compared to controls (Fig. 4). These results support the stimulation of
169 BC particle aggregation due to amino acid adsorption and their subsequent bacterial
170 colonization as depicted by nanoSIMS analyses (Fig. 1).
171 The structural and chemical reactivity characteristics of BC particles depend on the
172 combustion conditions that the original material experienced before becoming BC (Lehmann
173 et al., 2011), as well as on its abiotic degradation during atmospheric transportation and/or
174 subsequent deposition in seawater (Zimmerman, 2010). For example, UV radiation has been
175 observed to promote the oxidation of BC and the leakage of nutrients and organic molecules

176 in seawater enhancing bacterial activity (Malits et al., 2015). Hence, future experiments
177 should explore the variability of microbial BC colonization and remineralization according to
178 its structural and chemical characteristics. Finally, the colonizing microbial community may
179 be dynamic, with opportunistic microbial communities (*r*-strategists or rapidly reproducing
180 organisms typical of unstable environments) colonizing BC particles and degrading them
181 thanks to substrate primer availability, and specialist microbes (*k*-strategists or slowly
182 reproducing organisms typical of less variable environments) appearing later in the
183 degradation process as the BC particle becomes more refractory (Liang et al., 2010;
184 Zimmerman et al., 2011). The successional colonization of BC particles at sea remains to be
185 explored (Datta et al., 2016).
186 BC additions may induce changes in soil chemistry, affecting the composition and
187 metabolism of the microbial communities it contains, and overall carbon cycling in these
188 environments (Hill et al., 2019; Lehmann et al., 2011). Similarly, the microbial colonization
189 and remineralization of BC particles deposited at sea may contribute to carbon sequestration
190 in the ocean (Weinbauer et al., 2012), a process that remains undocumented despite the
191 important flux of BC to the oceans (Coppola et al., 2018; Jurado et al., 2008). The significant
192 proliferation of bacteria observed along the course of our experiments could imply that the
193 added amino acids acted as a priming effect, promoting the colonization of BC particles and
194 presumably their degradation. However, the bacterial colonization of BC observed here does
195 not imply that the particles were eventually remineralized, and bacteria could have been
196 merely attracted by the adsorbed amino acids. Further experiments measuring CO_2 release or
197 oxygen consumption are needed to verify if remineralization does actually happen when BC
198 particles are incubated with marine microbes and if it is facilitated by the availability of
199 organic molecules, as previously done in soil experiments (Hamer et al., 2004; Liang et al.,

2010). Such experiments will allow constraining the role of BC in the carbon pump and the extent to which it affects CO_2 sequestration by the oceans.

5. Conclusions

Current estimates of BC introduction into the ocean ascend to ~50 Tg C per year (Coppola et al., 2018; Jurado et al., 2008). This flux could impact the biological pump in unknown ways. While BC has been traditionally considered a refractory material unavailable for biological use, soil studies have documented BC particle bacterial remineralization in the presence of priming factors such as inorganic nutrients or organic molecules. Here we document the microbial colonization of BC particles in coastal seawaters off Vietnam, which occurred only in the presence of amino acids. Our results provide a step forward on our understanding of BC-microbial interactions in the ocean laying the ground for future studies constraining the impact of BC in the marine biological carbon pump.

Acknowledgements

This work was supported by the French National Research Institute for Sustainable Development (IRD) via an Action Sud grant awarded to M.B. and X.M, and by the International Research Network on the Impact of Black Carbon in South East Asia (SOOT-SEA). The authors would like to thank the MIO's team CYBELE for their support. We are indebted to R. Duhamel from the MNHN nanoSIMS facility for his assistance with image analyses. The electron microscopy experiments were performed by N. Brouilly and F. Richard on the PiCSL-FBI core facility (IBDM, Aix-Marseille University), member of the France-BioImaging national research infrastructure.

References

Benavides, M., Berthelot, H., Duhamel, S., Raimbault, P., Bonnet, S., 2017. Dissolved organic matter uptake by Trichodesmium in the Southwest Pacific. Sci. Rep. 7, 1–6. https://doi.org/10.1038/srep41315

Bond, T.C., Doherty, S.J., Fahey, D.W., Forster, P.M., Berntsen, T., Deangelo, B.J., Flanner, M.G., Ghan, S., Kärcher, B., Koch, D., Kinne, S., Kondo, Y., Quinn, P.K., Sarofim, M.C., Schultz, M.G., Schulz, M., Venkataraman, C., Zhang, H., Zhang, S., Bellouin, N., Guttikunda, S.K., Hopke, P.K., Jacobson, M.Z., Kaiser, J.W., Klimont, Z., Lohmann, U., Schwarz, J.P., Shindell, D., Storelvmo, T., Warren, S.G., Zender, C.S., 2013. Bounding the role of black carbon in the climate system: A scientific assessment. J. Geophys. Res. Atmos. 118, 5380–5552. https://doi.org/10.1002/jgrd.50171

Borges, A. V., Delille, B., Frankignoulle, M., 2005. Budgeting sinks and sources of CO2 in the coastal ocean: Diversity of ecosystem counts. Geophys. Res. Lett. 32, 1–4. https://doi.org/10.1029/2005GL023053

Cattaneo, R., Rouviere, C., Rassoulzadegan, F., Weinbauer, M.G., 2010a. Association of marine viral and bacterial communities with reference black carbon particles under experimental conditions: an analysis with scanning electron, epifluorescence and confocal laser scanning microscopy. FEMS Microbiol. Ecol. 74, 382–396. https://doi.org/10.1111/j.1574-6941.2010.00953.x

Cattaneo, R., Rouviere, C., Rassoulzadegan, F., Weinbauer, M.G., 2010b. Association ofmarineviral and bacterial communitieswith reference black carbon particles under experimental conditions: An analysiswith scanning electron, epifluorescence and confocal laser scanning microscopy. FEMS Microbiol. Ecol. https://doi.org/10.1111/j.1574-6941.2010.00953.x

Coppola, A.I., Wiedemeier, D.B., Galy, V., Haghipour, N., Hanke, U.M., Nascimento, G.S.,

Usman, M., Blattmann, T.M., Reisser, M., Freymond, C. V., Zhao, M., Voss, B., Wacker, L., Schefuß, E., Peucker-Ehrenbrink, B., Abiven, S., Schmidt, M.W.I., Eglinton, T.I., 2018a. Global-scale evidence for the refractory nature of riverine black carbon. Nat. Geosci. 11, 584–588. https://doi.org/10.1038/s41561-018-0159-8

Cunliffe, M., Wurl, O., 2014. Guide to best practices to study the ocean's surface, Scientific Committe on Oceanic Research.

Datta, M.S., Sliwerska, E., Gore, J., Polz, M.F., Cordero, O.X., 2016. Microbial interactions lead to rapid micro-scale successions on model marine particles. Nat. Commun. https://doi.org/10.1038/ncomms11965

Del Giorgio, P.A., Duarte, C.M., 2002. Respiration in the open ocean. Nature 420, 379–384. https://doi.org/10.1038/nature01165

Gao, S., DeLuca, T.H., Cleveland, C.C., 2019. Biochar additions alter phosphorus and nitrogen availability in agricultural ecosystems: A meta-analysis. Sci. Total Environ. https://doi.org/10.1016/j.scitotenv.2018.11.124

Hamer, U., Marschner, B., Brodowski, S., Amelung, W., 2004. Interactive priming of black carbon and glucose mineralisation. Org. Geochem. 35, 823–830. https://doi.org/10.1016/j.orggeochem.2004.03.003

Hill, R., Hunt, J., Sanders, E., Tran, M., Burk, G.A., Mlsna, T.E., Fitzkee, N.C., 2019. Effect of Biochar on Microbial Growth: A Metabolomics and Bacteriological Investigation in E. coli. Environ. Sci. Technol. acs.est.8b05024. https://doi.org/10.1021/acs.est.8b05024

Jurado, E., Dachs, J., Duarte, C.M., Simó, R., 2008. Atmospheric deposition of organic and black carbon to the global oceans. Atmos. Environ. 42, 7931–7939. https://doi.org/10.1016/j.atmosenv.2008.07.029

Lehmann, J., Rillig, M.C., Thies, J., Masiello, C.A., Hockaday, W.C., Crowley, D., 2011. Biochar effects on soil biota - A review. Soil Biol. Biochem. 43, 1812–1836.

https://doi.org/10.1016/j.soilbio.2011.04.022

Liang, B., Lehmann, J., Sohi, S.P., Thies, J.E., O'Neill, B., Trujillo, L., Gaunt, J., Solomon, D., Grossman, J., Neves, E.G., Luizão, F.J., 2010. Black carbon affects the cycling of non-black carbon in soil. Org. Geochem. 41, 206–213. https://doi.org/10.1016/j.orggeochem.2009.09.007

Liang, B., Lehmann, J., Solomon, D., Kinyangi, J., Grossman, J., O'Neill, B., Skjemstad, O., Thies, J., Luizao, F., Petersen, J., Neves, E., 2006. Black Carbon Increases Cation Exchange Capacity in Soils. Soil Sci. Soc. Am. J. 70, 1719. https://doi.org/10.2136/sssaj2005.0383

Malits, A., Cattaneo, R., Sintes, E., Gasol, J., Herndl, G., Weinbauer, M., 2015. Potential impacts of black carbon on the marine microbial community. Aquat. Microb. Ecol. 75, 27–42. https://doi.org/10.3354/ame01742

Mari, X., Chu Van, T., Guinot, B., Brune, J., Lefebvre, J.-P., Raimbault, P., Dittmar, T., Niggemann, J., 2017. Seasonal dynamics of atmospheric and river inputs of black carbon, and impacts on biogeochemical cycles in Halong Bay, Vietnam. Elem Sci Anth 5, 75. https://doi.org/10.1525/elementa.255

Mari, X., Lefèvre, J., Torréton, J., Bettarel, Y., Pringault, O., Rochelle-newall, E., Marchesiello, P., Menkes, C., Rodier, M., Migon, C., Motegi, C., Weinbauer, M.G., Legendre, L., Al, M.E.T., 2014a. Effects of soot deposition on particle dynamics and microbial processes in marine surface waters. Glob. Biogeochem. Cycles 662–678. https://doi.org/10.1002/2014GB004878.Received

Mari, X., Lefèvre, J., Torréton, J.P., Bettarel, Y., Pringault, O., Rochelle-Newall, E., Marchesiello, P., Menkes, C., Rodier, M., Migon, C., Motegi, C., Weinbauer, M.G., Legendre, L., 2014b. Effects of soot deposition on particle dynamics and microbial processes in marine surface waters. Global Biogeochem. Cycles.

https://doi.org/10.1002/2014GB004878

Masiello, C.A., 2004. New directions in black carbon organic geochemistry. Mar. Chem. 92, 201–213. https://doi.org/10.1016/j.marchem.2004.06.043

McBeath, A., Wynn, J.G., Wurster, C.M., Saiz, G., Bird, M.I., 2015. The Pyrogenic Carbon Cycle. Annu. Rev. Earth Planet. Sci. 43, 273–298. https://doi.org/10.1146/annurev-earth-060614-105038

OECD, 2016. The Economic Consequences of Outdoor Air Pollution 73–88. https://doi.org/10.1787/9789264257474-en

Pradeep Ram, A.S., Mari, X., Brune, J., Torréton, J.P., Chu, V.T., Raimbault, P., Niggemann, J., Sime-Ngando, T., 2018. Bacterial-viral interactions in the sea surface microlayer of a black carbon-dominated tropical coastal ecosystem (Halong Bay, Vietnam). Elem Sci Anth 6, 13. https://doi.org/10.1525/elementa.276

Rockne, K.J., Taghon, G.L., Kosson, D.S., 2000. Pore structure of soot deposits from several combustion sources. Chemosphere 41, 1125–1135. https://doi.org/10.1016/S0045-6535(00)00040-0

Weinbauer, M.G., Bettarel, Y., Cattaneo, R., Luef, B., Maier, C., Motegi, C., Peduzzi, P., Mari, X., 2009. Viral ecology of organic and inorganic particles in aquatic systems: Avenues for further research. Aquat. Microb. Ecol. 57, 321–341. https://doi.org/10.3354/ame01363

Weinbauer, M G, Cattaneo, R., Malits, A., Motegi, C., Gasol, J.M., Hernd, G.J., Mari, X., Migon, C., Rassoulzadegan, F., 2012. Black Carbon and Microorganisms in Aquatic Systems, Advances in Environmental Research. https://doi.org/10.1016/0304-3800(90)90021-8

Weinbauer, Markus G, Cattaneo, R., Malits, A., Motegi, C., Gasol, J.M., Herndl, G.J., Mari, X., Migon, C., Rassoulzadegan, F., 2012. Black Carbon and Microorganisms in Aquatic

Systems, Ecological Modelling. https://doi.org/10.1016/0304-3800(90)90021-8

Weinbauer, M.G., Guinot, B., Migon, C., Malfatti, F., Mari, X., 2017. Skyfall - neglected roles of volcano ash and black carbon rich aerosols for microbial plankton in the ocean. J. Plankton Res. 39, 187–198. https://doi.org/10.1093/plankt/fbw100

Wu, S., He, H., Inthapanya, X., Yang, C., Lu, L., Zeng, G., Han, Z., 2017. Role of biochar on composting of organic wastes and remediation of contaminated soils—a review. Environ. Sci. Pollut. Res. 24, 16560–16577. https://doi.org/10.1007/s11356-017-9168-1

Zerda, T.W., Xu, W., Zerda, A., Zhao, Y., Von Dreele, R.B., 2000. High pressure Raman and neutron scattering study on structure of carbon black particles. Carbon N. Y. 38, 355–361. https://doi.org/10.1016/S0008-6223(99)00111-6

Zimmerman, A.R., 2010. Abiotic and Microbial Oxidation of Laboratory- Produced Black Carbon (Biochar). Environ. Sci Technol. 44, 1295–1301. https://doi.org/10.1021/es903140c

Zimmerman, A.R., Gao, B., Ahn, M.Y., 2011. Positive and negative carbon mineralization priming effects among a variety of biochar-amended soils. Soil Biol. Biochem. 43, 1169–1179. https://doi.org/10.1016/j.soilbio.2011.02.005

Figure captions

Figure 1: NanoSIMS images of BC particles. ^{12}C enrichment of BC particles in control (not labelled, A) and ^{15}N-labeled amino acid samples after 12 h (B), 24 h (C) and 48 h (D) of incubation. Algal amino acid adsorption onto BC particles as depicted by the $^{15}N/^{14}N$ isotope ratio in control (E), and incubated samples (12, 24 and 48 h – F, G and H, respectively). Presence of bacteria as depicted by ^{31}P enrichment in control (I), and incubated samples (12, 24 and 48 h – J, K and L, respectively).

Figure 2: ^{15}N and ^{31}P enrichment of BC-amended seawater samples labelled with ^{15}N-labeled amino acids at 12, 24 and 48 h: (A) $^{15}N/^{14}N$ isotope ratio, (B) ^{31}P counts above an arbitrary threshold measured by the nanoSIMS. (C) Bacterial DAPI counts at the same time points. Dashed lines indicate the values of each variable measured in control samples at 48 h (not incubated with ^{15}N-labeled amino acids).

Figure 3: (A) SEM image of a BC particle in a control sample (not amended with ^{15}N-labeled amino acids). (B, C) Two examples of BC particles from samples incubated with ^{15}N-labeled amino acids after 48 h of incubation, showing bacterial biofilms (marked with red arrows).

Figure 4: Left two bottles: two replicate incubation bottles amended with 15N-labeled amino acids after 48 h of incubation, right bottle: control sample (not amended with 15N-labeled amino acids) after the same incubation period. The picture depicts how the addition of amino acids favoured BC particle aggregation (two left bottles), while in unamended samples BC tended to remain in dissolved form.

Control

12 h

24 h

48 h

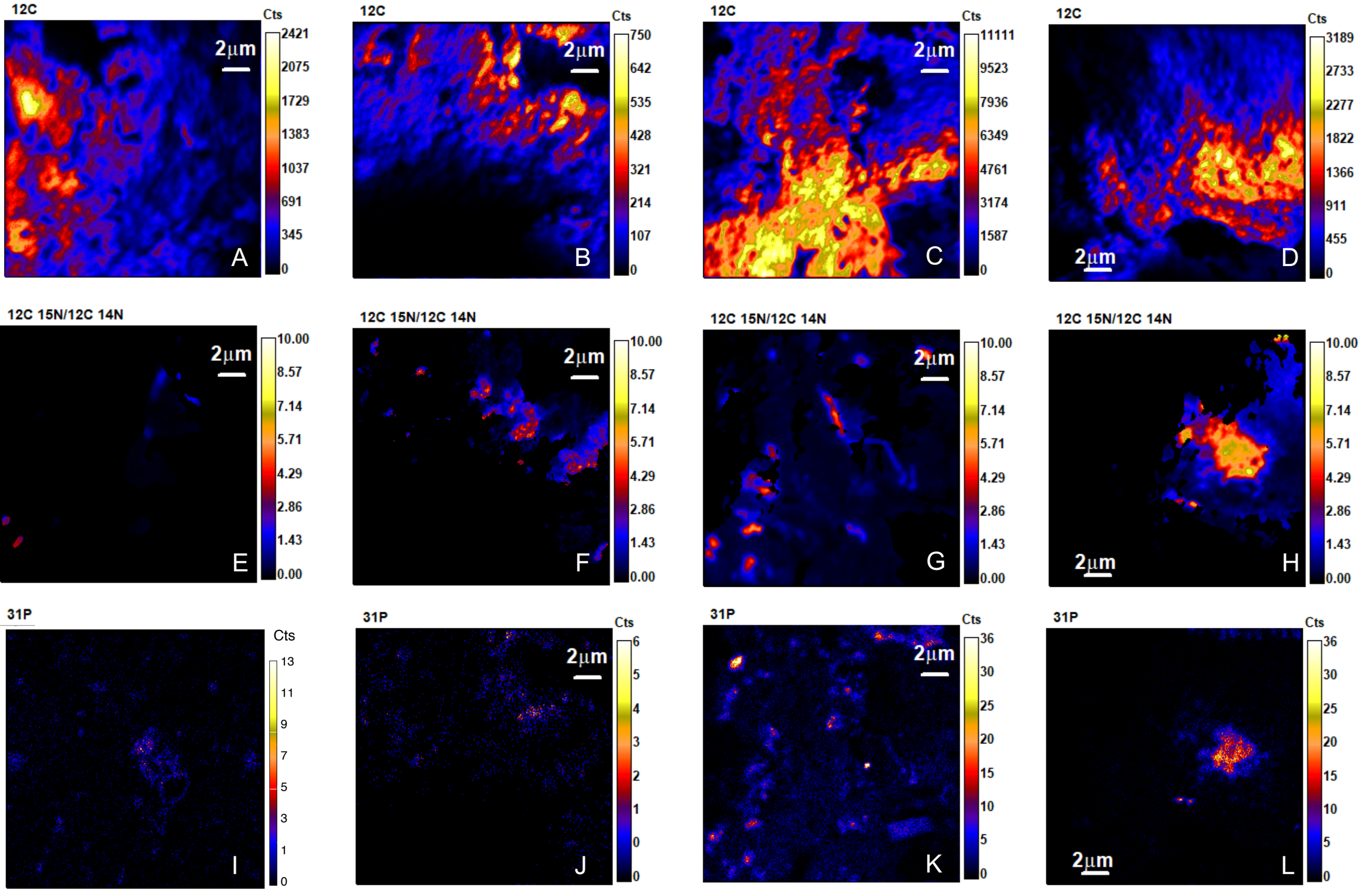

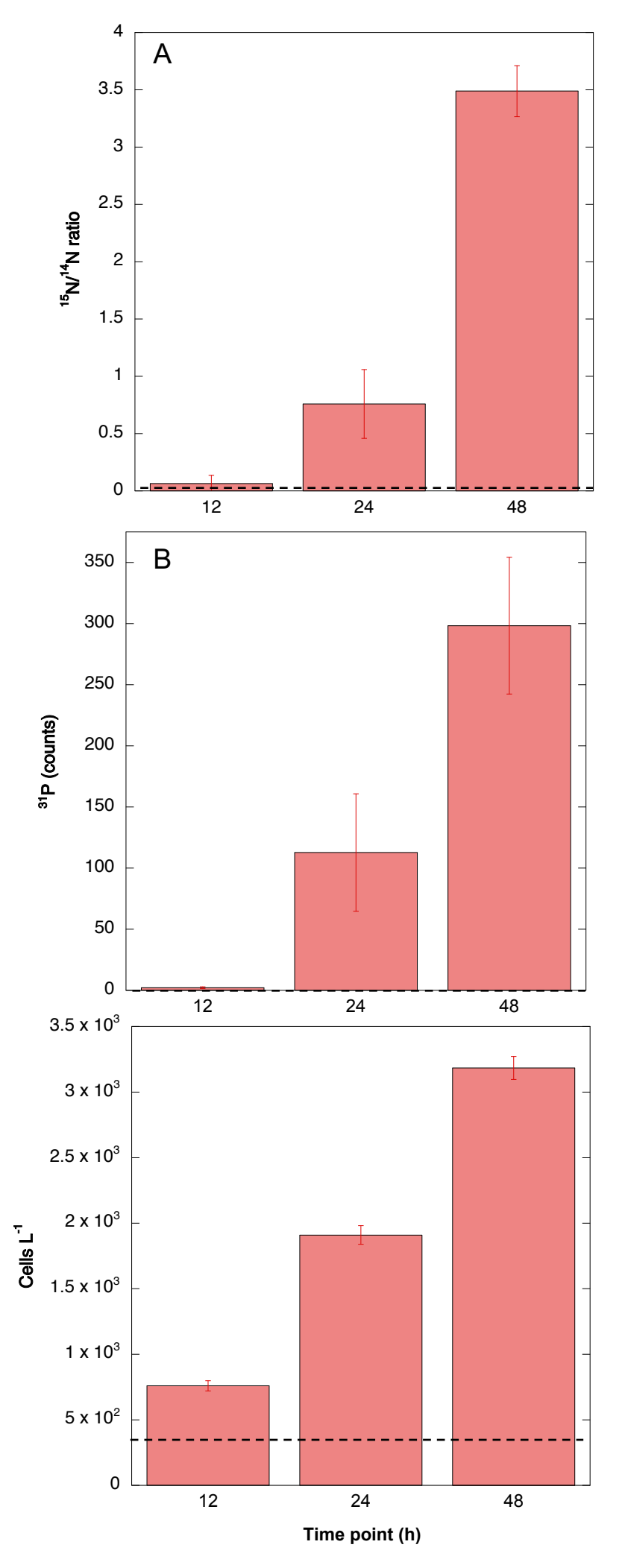
A
$^{15}N/^{14}N$ ratio
4
3.5
3
2.5
2
1.5
1
0.5
0
12
24
48
B
^{31}P (counts)
350
300
250
200
150
100
50
0
12
24
48
Cells L^{-1}
3.5×10^3
3×10^3
2.5×10^3
2×10^3
1.5×10^3
1×10^3
5×10^2
0
12
24
48
Time point (h)

A

x: 28.2557 mm	2/14/2019	HV	det	WD	HFW	mag	5 µm
y: 3.1198 mm	11:54:48 AM	10.00 kV	ETD	9.4 mm	15.9 µm	8 000 x	FEI Teneo

B

x: -23.3493 mm	3/12/2019	HV	det	WD	HFW	mag	2 µm
y: 18.3207 mm	11:22:51 AM	20.00 kV	ETD	5.4 mm	8.47 µm	15 000 x	FEI Teneo

C

x: -23.3704 mm	3/12/2019	HV	det	WD	HFW	mag	2 µm
y: 18.3827 mm	11:36:54 AM	20.00 kV	ETD	5.5 mm	8.47 µm	15 000 x	FEI Teneo


Benavides
Don. A
t48
Benavides
Don B
t48
Benavides
Don Cntrl
t48